Geophysical Research Letters

RESEARCH LETTER
10.1029/2020GL090095

A Hybrid Dynamical-Statistical Model for Advancing Subseasonal Tropical Cyclone Prediction Over the Western North Pacific

Yitian Qian[1], Pang-Chi Hsu[1], Hiroyuki Murakami[2,3], Baoqiang Xiang[2,3], and Lijun You[4]

[1]Key Laboratory of Meteorological Disaster of Ministry of Education/Joint International Research Laboratory of Climate and Environment Change/Collaborative Innovation Center on Forecast and Evaluation of Meteorological Disasters, Nanjing University of Information Science and Technology, Nanjing, China, [2]National Oceanic and Atmospheric Administration/Geophysical Fluid Dynamics Laboratory, Princeton, NJ, USA, [3]University Corporation for Atmospheric Research, Boulder, CO, USA, [4]Fujian Key Laboratory of Severe Weather, Fujian Meteorological Bureau, Fuzhou, China

Key Points:
- A hybrid dynamical-statistical model for predicting tropical cyclone frequency and trajectory at the subseasonal timescale was developed
- Significant skill can be achieved with a forecast lead time of 25 days
- The prediction skill of this hybrid model is superior to the statistical and dynamical model-based predictions examined in this study

Supporting Information:
- Supporting Information S1

Correspondence to:
P.-C. Hsu,
pangchi@nuist.edu.cn

Citation:
Qian, Y., Hsu, P.-C., Murakami, H., Xiang, B., & You, L. (2020). A hybrid dynamical-statistical model for advancing subseasonal tropical cyclone prediction over the western North Pacific. *Geophysical Research Letters*, *47*, e2020GL090095. https://doi.org/10.1029/2020GL090095

Received 31 JUL 2020
Accepted 12 OCT 2020
Accepted article online 17 OCT 2020

Abstract Tropical cyclone (TC) genesis prediction at the extended-range to subseasonal timescale (a week to several weeks) is a gap between weather and climate predictions. The current dynamical prediction systems and statistical models show limited skills in TC genesis forecasting at the lead time of 1–3 weeks. A hybrid dynamical-statistical model is developed that reveals capability in predicting basin-wide TC frequency in every 10-day period over the western North Pacific at a 25-day forecast lead, which is superior to the statistical and dynamical model-based predictions examined in this study. In this hybrid model, the cyclogenesis counts for different TC clusters are predicted, respectively, using the statistical models in which the large-scale predictors associated with intraseasonal oscillation evolutions are provided by a dynamical model. A probabilistic map of TC tracks at the subseasonal timescale is further predicted by incorporating the climatological probability of track distributions of these TC clusters.

Plain Language Summary Tropical cyclone (TC) is a highly destructive type of natural disaster. Extending forecast lead times and increasing the forecast accuracy of TC genesis and movements are the keys for disaster prevention and mitigation. However, TC predictions at the subseasonal timescale (10 days to several weeks in advance) have not reached a satisfactory level. Most dynamical prediction systems and statistical models show skills of 1–3 weeks for subseasonal TC genesis prediction. In this study, we developed a hybrid dynamical-statistical prediction approach for advancing the capability to predict TC frequency over the western North Pacific (WNP). Considering the close linkage between intraseasonal oscillation and WNP TC genesis, multiple linear regression models in which the intraseasonal dynamic and thermodynamic conditions serve as the predictors were constructed for different TC clusters over the WNP. We find that future TC genesis counts can be predicted once we obtain the information on intraseasonal predictors from a dynamical prediction system. This hybrid model shows good skills for basin-wide TC genesis prediction at the forecast lead time of 25 days, and is superior to the statistical and dynamical model-based predictions examined in this study. In addition, a probabilistic map of WNP TC trajectories is also skillfully predicted at the subseasonal timescale.

1. Introduction

As one of the most extreme weather events, tropical cyclones (TCs) pose a major threat to people's lives and property in TC-prone coastal regions. Substantial progress has been made by the research community and at operational centers in terms of providing skillful predictions of TC activity at medium-range (up to 10 days) and seasonal (3–6 months) timescales. However, TC prediction at the extended-range to subseasonal timescale (a week to several weeks) remains a gap between medium-range weather forecast and seasonal prediction (Vitart et al., 2012; Waliser, 2011), primarily due to the lack of, and underutilized, sources of predictability at this intermediate timescale.

Earlier works on TC prediction at the subseasonal timescale were mainly based on statistical forecast models. For instance, using the real-time multivariate Madden-Julian Oscillation (MJO) index (i.e., RMM1 and RMM2), the two leading modes of Indo-Pacific sea surface temperature (SST) variability, and

information on climatological TC activity, Leroy and Wheeler (2008) developed a multiple logistic regression model to predict weekly TC activity in the Southern Hemisphere. A similar approach was later applied to TC prediction over the eastern Pacific and Atlantic basins by Slade and Maloney (2013). Their results showed that the MJO serves as an important source of predictability; a higher skill could be achieved (out to a 2-week forecast lead) when the RMM indices were included as predictors.

The improvements of dynamical models in predicting the intraseasonal oscillation (ISO) and its relationship with TCs suggest the possibility of predicting TCs at the subseasonal timescale (Gregory et al., 2020; Jiang et al., 2018; Lee et al., 2018, 2020; Vitart et al., 2010; Xiang et al., 2015). Vitart et al. (2010) indicated that the monthly forecast system of the European Centre for Medium-Range Weather Forecasts (ECMWF) was able to predict the weekly TC occurrence in the Southern Hemisphere at the forecast lead time of 2 weeks, as displayed by the logistic regression model in Leroy and Wheeler (2008). With a skillful MJO prediction out to 27 days (Xiang et al., 2015), the updated high-resolution (50-km) coupled Global Climate Model (GCM) of the Geophysical Fluid Dynamics Laboratory (GFDL) realistically predicted two destructive landfalling TCs over the Atlantic and Pacific about 11 days in advance (Xiang, Zhao, et al., 2015). Jiang et al. (2018) extended the work of Xiang, Zhao, et al. (2015) to assess the subseasonal TC genesis prediction skill for about 600 TC cases predicted by the same GFDL model; they found that only 10% of cyclogenesis events could be predicted at and beyond the 1-week forecast lead. Using the subseasonal-to-seasonal (S2S) prediction data set (Vitart et al., 2017), Lee et al. (2018) documented that only a few of the six S2S models showed skills for TC genesis prediction with the 2-week (8–14 days) forecasts. Gregory et al. (2020) and Lee et al. (2020) extended the work of Lee et al. (2018) to assess prediction skills of probabilistic TC occurrence at a regional scale (15° latitude × 20° longitude) over different basins. They concluded that the ECMWF model and the prediction systems from Australia and France show good skills in predicting the probability of TC occurrence out to 3–4 weeks in advance. Additional progresses of subseasonal TC prediction can be found in the review paper of Camargo et al. (2019).

The literatures reviewed above suggest that the state-of-the-art dynamical and statistical models still only have limited deterministic skills (1 to 2 weeks) in TC genesis number prediction at the subseasonal timescale. Considering the significant statistical relationship between western North Pacific (WNP) TC genesis and ISO-related dynamic and thermodynamic conditions (Camargo et al., 2009; Hsu et al., 2011; Zhao et al., 2015), and the improved skills in MJO prediction by dynamical models (Xiang, Lin, et al., 2015), we propose a hybrid dynamical-statistical approach to predict basin-wide TC occurrence frequency. In addition to cyclogenesis prediction, a probabilistic map of TC trajectories is also predicted by involving the climatological track patterns of WNP TC clusters from observations (Kim et al., 2012).

2. Data and Validation Methods

2.1. Observational Data

The TC data for the period 1979–2013 were obtained from the U.S. Department of Defense Joint Typhoon Warning Center (JTWC) Best Track Database. We focused on the TCs with tropical storm intensity or higher (wind speed ≥34 kt). Other data used included large-scale thermodynamic and dynamic environments related to TC genesis, including daily SST, zonal and meridional winds at 850 and 200 hPa, vertical velocity at 500 hPa, and specific humidity at 700 hPa from the ERA-Interim reanalysis data set (Dee et al., 2011), and daily outgoing longwave radiation (OLR) from the National Oceanic and Atmospheric Administration (NOAA) polar-orbiting satellites (Liebmann & Smith, 1996). All the large-scale fields were regridded to a horizontal resolution of 2.5° × 2.5° before analysis.

2.2. Dynamical Model and Hindcast Data

The dynamical model used in this study is the Forecast-Oriented Low Ocean Resolution (FLOR) version of the GFDL coupled model (Vecchi et al., 2014) with a newly developed double-plume convection scheme (Zhao et al., 2018). It showed a 27-day lead forecast skill for the MJO in the wintertime (Xiang, Lin, et al., 2015). For the boreal summer ISO over the WNP, it shows skills in predicting the evolution of dominant ISO modes at 15-day forecast lead and the spatial distributions of intraseasonal convection, circulation, and SST anomalies up to 40-day forecast lead (supporting information Text S1, Figure S1). This model has a horizontal resolution of 50 km with 32 vertical levels. Using a nudging technique toward observations to obtain initial conditions (Xiang, Lin, et al., 2015), hindcasts were carried out every

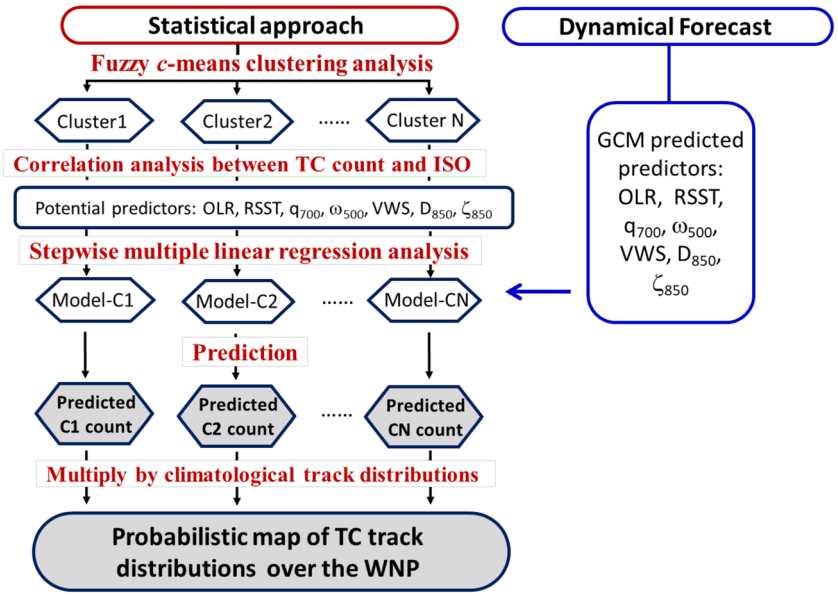

Figure 1. A flowchart summarizing the procedures to construct the hybrid dynamical-statistical model for subseasonal TC genesis counts and trajectory predictions.

5 days (the 1st, 6th, 11th, 16th, 21st, and 26th) for each month from April to November during the 11 years of 2003–2013. For the hindcasts initialized on each day, a series of 50-day integrations with initial conditions every 4 hr (i.e., at 0000, 0400, 1600, and 2000 UTC) constituted six ensemble members. Thus, in total there were 3,168 hindcasts (11 years × 8 months × 6 days × 6 members) produced. Xiang, Zhao, et al. (2015) and Jiang et al. (2018) detected TC geneses using the same hindcast data (Text S2). Thus, the skills in TC genesis prediction derived directly from this dynamical model and from our hybrid model can be compared.

2.3. Skill Scores

Temporal correlation coefficient (TCC) and root-mean-square error (RMSE) are adopted to measure deterministic prediction skills

$$\mathrm{TCC}(\tau)=\frac{\sum_{t=1}^{T}\left(p_t(\tau)-\overline{p(\tau)}\right)(o_t-\overline{o})}{\sqrt{\sum_{t=1}^{T}\left(p(\tau)_t-\overline{p(\tau)}\right)^2}\sqrt{\sum_{t=1}^{T}(o_t-\overline{o})^2}} \tag{1}$$

and

$$\mathrm{RMSE}(\tau)=\sqrt{\frac{1}{T}\sum_{t=1}^{T}\left(p(\tau)_t-o_t\right)^2}. \tag{2}$$

Here τ represents the forecast lead time, p_t and o_t are the predicted and observed TC genesis frequency at the tth 10-day period, respectively, during the independent forecast period with T 10-day periods ($T=220$). $\overline{p}$ and $\overline{o}$ are the averages of predicted and observed TC genesis counts over the forecast period, respectively.

The relative operating characteristic (ROC; Stanski et al., 1989) score, defined as the area below the ROC curve (area under curve, or AUC), is used to assess the probabilistic prediction results (Vitart et al., 2010). The ROC curve is formed by dotting the hit rates (y axis) against false-alarm rates (x axis) of TC genesis for different probability thresholds with an interval of 0.2. A perfect prediction is achieved when the AUC is equal to 1.0, while a no-skill forecast is called when an AUC is 0.5 or smaller. Although the ROC diagram provides information about the capability of the forecast to distinguish between several events with different

outcomes, it is not sensitive to prediction biases (Jolliffe & Stephenson, 2005) like reliability or attributes diagram (Wilks, 2006; Zhang et al., 2019).

3. Hybrid Model Construction and its Prediction Results

3.1. Steps for Developing the Subseasonal TC Prediction Model

The basin-total TC counts and probabilistic map of TC tracks over the WNP (100–180°E, 0–60°N) in every 10-day period during the TC season (16 May to 5 December; twenty 10-day periods in each year) were predicted at the forecast leads of 10–40 days. Figure 1 illustrates the major procedures of the hybrid dynamical-statistical prediction approach in our study. Similar to the track-pattern-based model for seasonal TC track-density prediction proposed by Chu et al. (2010), Kim et al. (2012), and Murakami et al. (2016), we objectively classify the WNP TCs into seven track patterns by using the fuzzy *c*-mean clustering method as several studies suggested that the optimum cluster number for the WNP TC activity is seven (Camargo et al., 2007; Kim et al., 2011). Given the fact that each TC cluster reveals distinct genesis locations and trajectories (Figure 2), one can predict the TC tracks by applying the observational climatological track pattern once the genesis count of individual clusters is known. In this study, the anomalous TC genesis counts of individual clusters relative to their annual cycles (climatological 10-day-period mean) are predicted by statistical models in which the predictors are obtained from dynamical predictions. The basin-wide TC genesis numbers are then obtained from the summation of predicted anomalous TC counts and their annual cycles for all seven clusters. We used 24 TC seasons from 1979–2002 as the training period to construct the statistical models based on the concurrent relationships between TC (from the JTWC best-track data) and large-scale convection and circulation fields (from the NOAA OLR and ERA-Interim data sets) associated with the ISO. An independent forecast was carried out for the 11 TC seasons of 2003–2013 by utilizing the predicted large-scale fields from the GFDL FLOR model for validation against the observations. There are 220 (twenty 10-day periods × 11 years) and 480 (twenty 10-day periods × 24 years) time points for prediction in the independent forecast period and training period, respectively.

To examine the sources of predictability, we first carried out a spectral analysis of the time series of anomalous TC genesis counts (Figure 2). As we can see, there are significant peaks in the spectrum at the intraseasonal timescale from 20 to 90 days for individual TC clusters (Figures 2a–2g) and all TC cases (Figure 2h). This suggests that the ISO activities are one of the key factors exerting influences not only on the overall WNP TC activity (Camargo et al., 2009; Hsu et al., 2011; Li & Zhou, 2013; Zhao et al., 2015) but also on individual TC patterns. In other words, the ISO may provide predictability for subseasonal TC genesis predictions (Jiang et al., 2018; Lee et al., 2018; Leroy & Wheeler, 2008; Vitart et al., 2010) for these distinct clusters. Therefore, the intraseasonal large-scale thermodynamic and dynamic environments, such as OLR, SST, specific humidity at 700 hPa (q_{700}), vertical velocity at 500 hPa (ω_{500}), zonal vertical wind shear between 200 and 850 hPa (VWS), divergence at 850 hPa (D_{850}), and relative vorticity at 850 hPa (ζ_{850}), which physically modulate the subseasonal variation of TC genesis (Camargo et al., 2009; Zhao et al., 2015), were selected to serve as the potential predictors. Note that for real-time application, the intraseasonal component of each predictor is derived using a nonbandpass-filtering method (Hsu et al., 2015; Qian et al., 2019; Wheeler & Hendon, 2004). First, the low-frequency background state is removed by subtracting the climatological mean and first three harmonics of climatological annual variation from the observed raw data of the ERA-Interim and NOAA OLR. Then, a 10-day average is applied to remove the high-frequency signals and also to obtain the predictors in every 10-day interval.

As seen in the correlation maps between anomalous TC counts of Cluster One (C1) and large-scale ISO fields (Figure S2), TC formations associated with different clusters are modulated by ISO-related background environments to varying degrees. To reduce the uncertainty of predictor selections, four methods were utilized to identify the key signals that can be used as efficient and reliable predictors (Text S3, Figure S2). Then, the statistical models based on the stepwise multiple linear regression analysis were developed to predict the genesis counts in each 10-day period of individual TC clusters. The multiple linear regression forecast model for anomalous TC genesis counts (y) is expressed as follows:

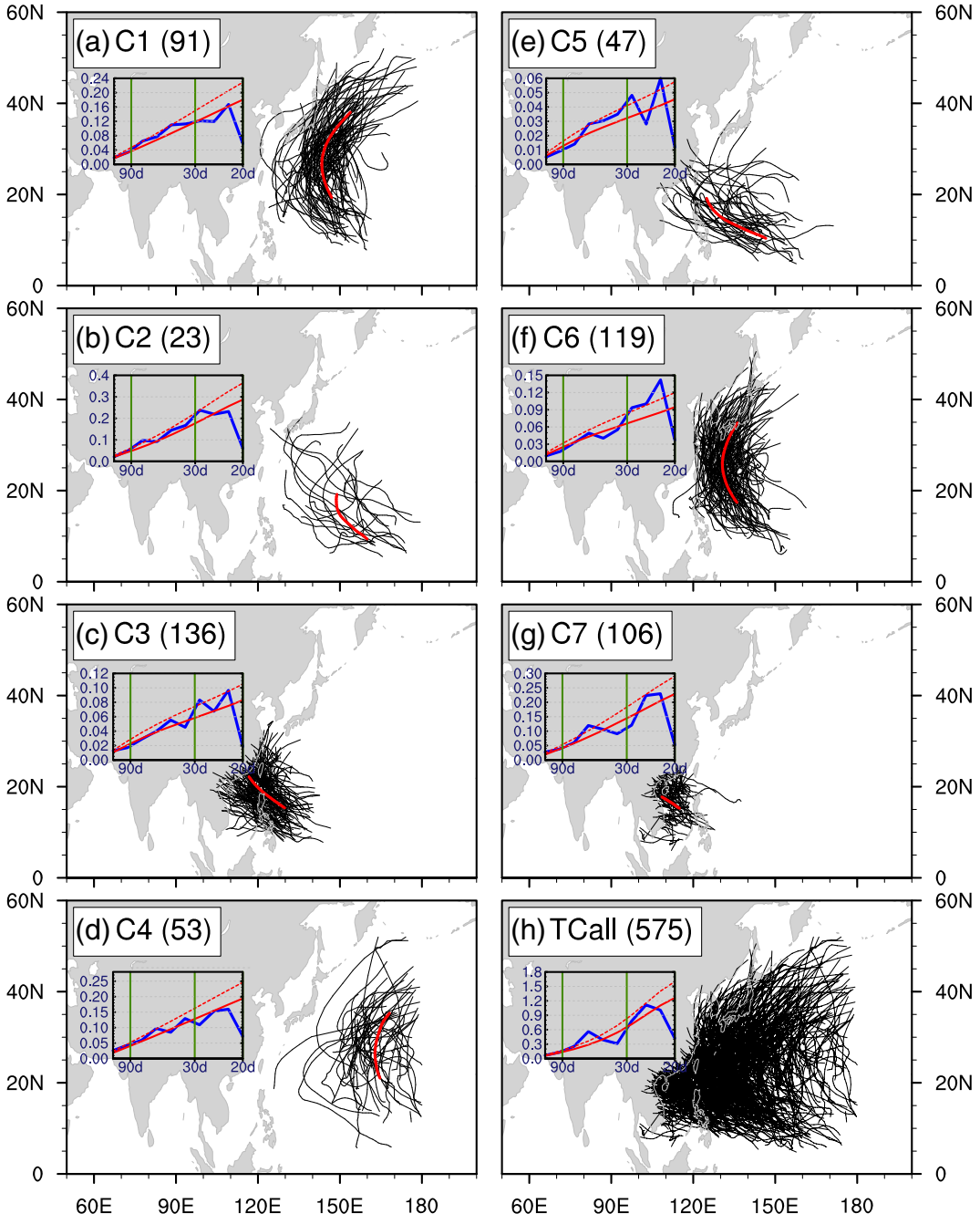

Figure 2. Seven clusters of WNP TCs classified using the fuzzy *c*-means clustering method. (a–g) TC trajectories (black lines) and their central trajectories (red lines) for each of the cluster patterns of C1 to C7. (h) Trajectories of all TCs over the WNP. The clustering analysis was applied to TC events during the TC seasons of the training period (1979–2002). The number in the parentheses of each panel indicates the TC count of each cluster. Spectral analysis of TC genesis counts (blue line) is also shown in each panel. Solid and dashed red lines represent the red noise spectrum and its 90% confidence level, respectively. Vertical green lines mark the periods of 30 and 90 days, respectively.

$$y = \beta_0 + \sum_{i=1}^{k} \beta_i x_i, \tag{3}$$

where k predictors and $k + 1$ parameters (β_i values) are selected by stepwise regression analysis from the potential predictors. The results of selected predictors for each cluster based on each of the four methods are shown in Table S1.

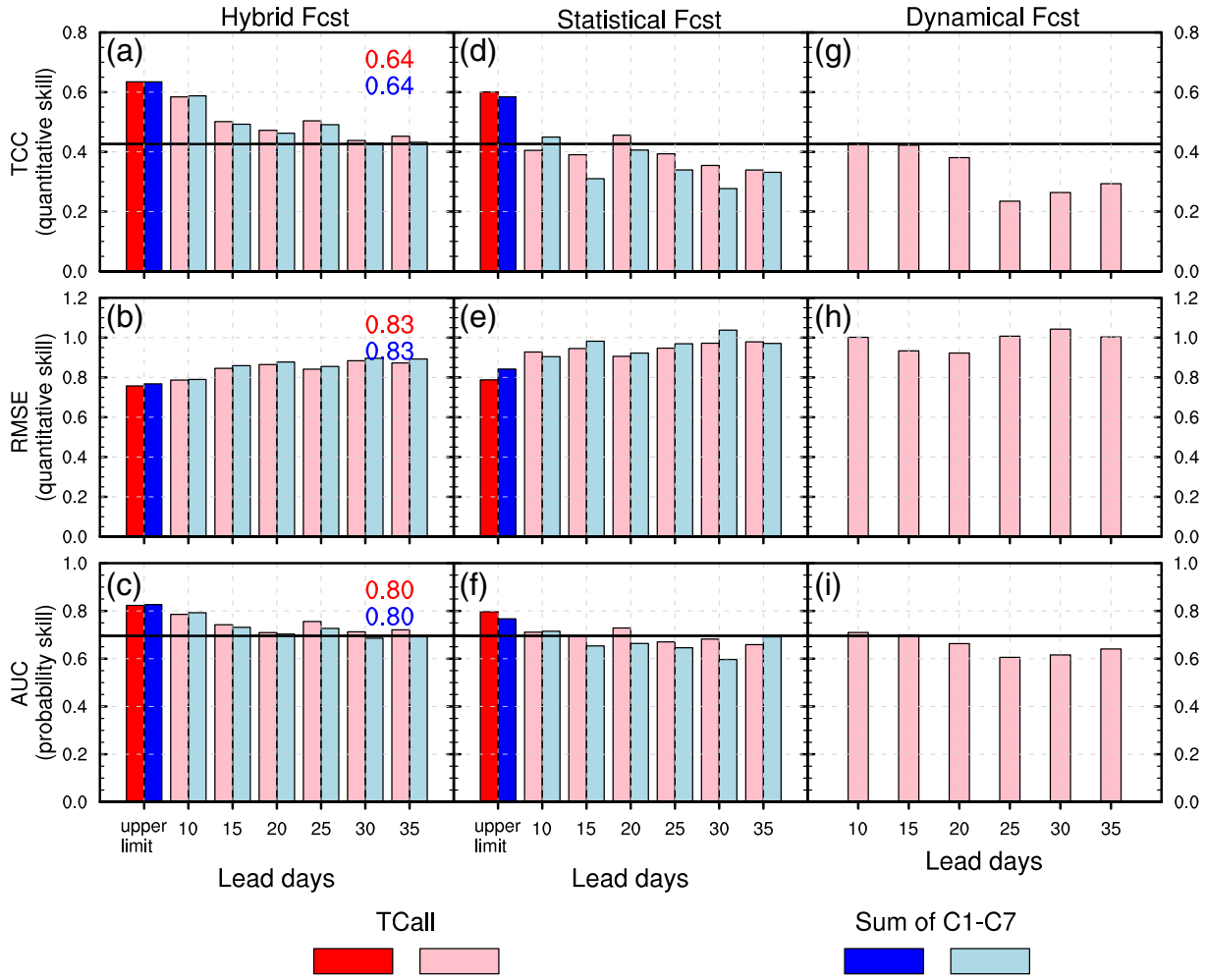

Figure 3. Basin-total TC count prediction skills of the hybrid model (left), statistical model (middle), and dynamical model (right). The prediction skill is evaluated by the (a, d, g) temporal correlation coefficients (TCC), (b, e, h) root-mean-square error (RMSE), and (c, f, i) area under the ROC curve (AUC) of the predicted TC counts against the observations during 2003–2013. Dark red and blue bars represent the predicted results using the observational predictors at the 0-day lead obtained from the sum of the C1–C7 TC counts and from the direct prediction of TCall, respectively, which is the upper limit of the statistical model. Pink and light blue bars indicate the prediction results obtained from the sum of the C1–C7 TC counts and from the direct prediction of TCall, respectively. The black line (TCC = 0.42 and AUC = 0.69) in (a, d, g) and (c, f, i) marks the climatological prediction skill. The red and blue numbers at the upper-right corner of (a)–(c) (using the same colors as the bars) represent the scores of statistical model fitting results (or the prediction of 0-day forecast lead) during the training period (1979–2002).

Using the large-scale ISO-related predictors in the future 40 days predicted by the GFDL coupled model, the TC genesis counts (y) of each cluster can be obtained. To derive the predicted ISO components, the predicted climatological daily mean as a function of start date and lead day was subtracted from the raw data. A 10-day average on the same dates as those in observations was then applied to remove high-frequency disturbances. Once the anomalous TC counts were predicted, we added the observed climatological mean of 10-day-period TC counts to obtain the total genesis counts in each 10-day period (future one to four 10-day periods) for each cluster. Then, the probability of TC track distributions in each 10-day period was derived by involving the climatology of each track probability (Text S4).

3.2. TC Genesis and Trajectory Prediction Results

The prediction skills for basin-total TC counts performed by the models for individual clusters (C1–C7 and their sum) and for the total cases (TCall) are assessed based on the chosen skill-score metrics, i.e., TCC, RMSE, and AUC (Figures 3 and S3). The upper limits of the statistical model's skills can be obtained as the predictors are from the 10-day periods of observations (instead of dynamical model predictions), which could be considered as the lead 0-day prediction. We first compared the prediction skills for anomalous TC

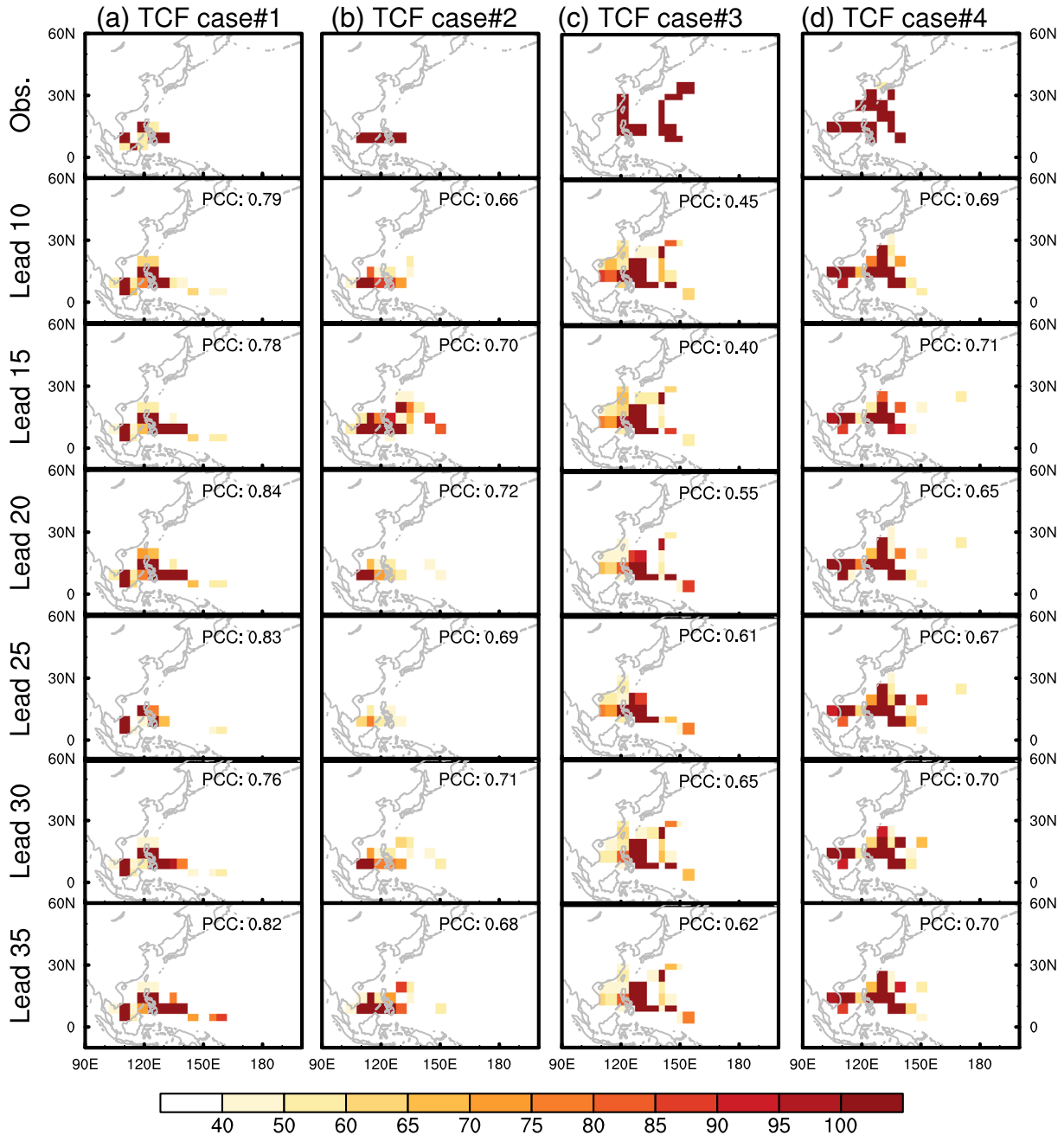

Figure 4. Observed (top panels) and predicted spatial patterns of TC frequency probability over the WNP at the forecast lead times of 10–35 days (six lower panels). (a, b) Two cases of high TC frequency (TCF) probability (units: %) over the Philippine Sea and South China Sea. (c–d) Two cases of predictions for recurving TCs. The TCF probability in each grid cell is defined as the TCF in each 5° × 5° box divided by the total TC count over the WNP. The PCC skill between predicted and observed TCFs is shown at the upper-right corner of each panel.

counts using hybrid models with predictors defined by the four different methods. The results were not sensitive to the methods (Figure S3). At the forecast lead of 10 days, all the hybrid models showed skills close to the forecast upper limits. Although the skills drop as the lead time become longer, the models are generally skillful in terms of TCC (AUC) out to 25-day (30-day) forecast leads (Figure S3). Owing to the similar results, the average of the predictions based on the four methods was adopted as an ensemble prediction. After adding the climatological mean of 10-day-period TC counts (Figure S5), the basin-total TC counts are predicted with TCC skill above 0.42 (i.e., the skill score performed by climatological prediction) beyond the 25-day forecast lead (Figure S4). To verify whether our statistical models were

overfitted, a series of tests related to the sources of overfitting were carried out, including the uncertainty of data sample, selection bias, and autocorrelation (Text S5). All the test results suggested that our statistical model performances are fairly robust without overfitting issue.

The superiority of this hybrid model can be seen from the comparison of its prediction skills with those of the dynamical prediction system (Text S2) and the purely statistical model (Text S6). The ensemble prediction of basin-total TC counts by the hybrid model shows a TCC skill out to 25-day forecast lead (Figure 3a), while the TCC skills are limited to about 10 days for both the statistical and dynamical models (Figures 3d and 3g). The RMSEs (AUCs) of the hybrid model prediction are also lower (higher) than those displayed by the statistical and dynamical models (middle and bottom panels in Figure 3). The deterministic prediction of TC genesis numbers over the WNP may supplement the information of TC genesis probability predicted by the ensemble system of the S2S models (Lee et al., 2018).

Although the prediction skills regarding TC counts for individual clusters are similar to those of TCall (Figure 3), the predicted TC genesis counts are useful for constructing probabilistic maps of TC frequency (TCF) over the WNP by involving the climatological probability of TC tracks in each cluster (Kim et al., 2012; see Text S4 for more detail). The climatological mean and standard deviations of the probabilistic maps for TCF derived from observations and hybrid model predictions are shown in Figure S8. The high pattern correlation coefficients (PCCs) between model predictions and observations indicate that this track pattern-based method (Text S4) has reasonable capability in reproducing the spatial characteristics of TCF probability over the WNP (Figure S8). The averaged PCC skill over the independent forecast period is significant at the forecast lead time of 35 days (Figure S9). To reveal the skill with respect to TCF predictions, we show in Figure 4 some cases of TCF probabilistic maps predicted at different lead times. For example, the high probabilities of TCs occurring over the Philippine Sea and South China Sea (cases 1 and 2) are predicted by the model at the lead time of 30 days (Figures 4a and 4b). The recurving trajectories of TCs approaching Japan and the Korean Peninsula are also predicted at a long lead (Figures 4c and 4d). The recent study of Lee et al. (2020) found that some S2S models are skillful in predicting regional TCF (in every 15° × 20° grid cell) at a long lead time out to 4 weeks based on the assessment of Brier skill score. Because the definition of track density based on the method of track-pattern-based model (Chu et al., 2010) is different from the probability of TCF of Lee et al. (2020), it is not yet clear whether our finer resolution (5° × 5°) prediction of TC density outperforms the dynamical prediction of the S2S models.

4. Summary and Discussion

Subseasonal prediction of TC activity has been challenging, while the state-of-the-art dynamical prediction systems show skills in the probabilistic predictions of TC occurrence anomalies with positive Brier skill scores at forecast leads up to 2–4 weeks over some basins (Gregory et al., 2020; Lee et al., 2018, 2020). Compared to the probabilistic prediction, the deterministic cyclogenesis (for both the location and time of TC genesis) prediction at the subseasonal timescale is much more difficult (Jiang et al., 2018). Only 10% of WNP TC geneses are predicted reasonably by one GFDL coupled model prediction system (Jiang et al., 2018). In this study, we developed a hybrid dynamical-statistical model to predict TC genesis counts over the WNP for different TC clusters in every 10-day period, and then constructed probability maps of TC tracks. Based on the modulating effects of ISO on WNP TC genesis, stepwise multiple linear regression models for individual clusters were developed, and the large-scale intraseasonal predictors used in the statistical models were incorporated from the predictions of the GFDL coupled model, which has capability in predicting the boreal summer ISO conditions related to TC genesis at leads of 15–40 days. Based on assessments of an 11-year independent forecast, these hybrid models show skillful predictions of total-basin TC genesis counts at the lead time of 25 days, which is superior to the statistical regression models based on the preceding intraseasonal fields as the predictors (purely statistical prediction) or the GFDL dynamical prediction system (purely dynamical prediction). The probabilistic map of TCF is also reasonably predicted at the subseasonal timescale.

The results of hybrid model prediction are promising, which benefit from the skillful predictions of ISO from the hindcast of the GFDL coupled model. For operational application, real-time prediction data of large-scale predictors are needed. In this respect, the S2S project provides a vital data set for further establishing a real-time TC prediction system based on our hybrid model prediction approach. Moreover, the ensemble members of the S2S prediction system can be efficiently used for probabilistic TC predictions, which

provide information on the uncertainty of the forecasts (Gregory et al., 2020; Lee et al., 2018, 2020). We are working with operational centers in TC-prone areas of China to advance this work. To improve the model skill, other useful predictors, such as high-frequency equatorial waves (Frank & Roundy, 2006; Schreck et al., 2012) and extratropical signals (Li et al., 2018; Zhang et al., 2017), are worthy further exploration. For understanding the skill of the current model with respect to the other prediction systems, developing a unified framework for definitions and validations of subseasonal TC prediction skill is also urgently needed (Camargo et al., 2019).

Data Availability Statement

The data used to construct the hybrid models with different four methods and the GFDL model predicted large-scale predictors for WNP TC predictions at the subseasonal timescale are available online (https://zenodo.org/record/4072444#.X36DJ1czabg). The ERA-Interim reanalysis data are available from the ECMWF (https://www.ecmwf.int/en/forecasts/datasets/), and the OLR data are available from NOAA (https://psl.noaa.gov/data/gridded/data.interp_OLR.html). The tropical cyclone data are from the U.S. Department of Defense Joint Typhoon Warning Center (JTWC) Best Track Database (https://www.metoc.navy.mil/jtwc/jtwc.html?western-pacific).

Acknowledgments
The authors would like to thank the anonymous reviewers for their comments, which helped improve the manuscript. The dynamical predictions of large-scale fields and tropical cyclones were conducted by using the Forecast-Oriented Low Ocean Resolution version of the GFDL coupled model. This work was supported by the National Key R&D Program of China (2018YFC1505805).

References

Camargo, S. J., Camp, J., Elsberry, E. L., Gregory, P. A., Klotzbach, P. J., Schreck, C. J., et al. (2019). Tropical cyclone prediction on sub-seasonal time-scale. *Tropical Cyclone Research and Review*, *8*, 150–165. https://doi.org/10.6057/2019TCRR03.04

Camargo, S. J., Robertson, A. W., Gaffney, S. J., Smyth, P., & Ghil, M. (2007). Cluster analysis of typhoon tracks. Part I. General properties. *Journal of Climate*, *20*(14), 3635–3653. https://doi.org/10.1175/JCLI4188.1

Camargo, S. J., Wheeler, M. C., & Sobel, A. H. (2009). Diagnosis of the MJO modulation of tropical cyclogenesis using an empirical index. *Journal of the Atmospheric Sciences*, *66*(10), 3061–3074. https://doi.org/10.1175/2009JAS3101.1

Chu, P.-S., Kim, C.-H., Kim, H.-S., Lu, M.-M., & Kim, J.-H. (2010). Bayesian forecasting of seasonal typhoon activity: A track-pattern-oriented categorization approach for Taiwan. *Journal of Climate*, *23*(24), 6654–6668. https://doi.org/10.1175/2010JCLI3710.1

Dee, D. P., Uppala, S. M., Simmons, A. J., Berrisford, P., Poli, P., Kobayashi, S., et al. (2011). The ERA-Interim reanalysis: Configuration and performance of the data assimilation system. *Quarterly Journal of the Royal Meteorological Society*, *137*(656), 553–597. https://doi.org/10.1002/qj.828

Frank, W. M., & Roundy, P. E. (2006). The role of tropical waves in tropical cyclogenesis. *Monthly Weather Review*, *134*(9), 2397–2417. https://doi.org/10.1175/MWR3204.1

Gregory, P., Vitart, F., Rivett, R., Brown, A., & Kuleshov, Y. (2020). Subseasonal forecasts of tropical cyclones in the Southern Hemisphere using a dynamical multimodel ensemble. *Weather and Forecasting*, *35*, 1817–1829. https://doi.org/10.1175/WAF-D-20-0050.1

Hsu, P.-C., Li, T., & Tsou, C.-H. (2011). Interactions between boreal summer intraseasonal oscillations and synoptic-scale disturbances over the western North Pacific. Part I: Energetics diagnosis. *Journal of Climate*, *24*(3), 927–941. https://doi.org/10.1175/2010JCLI3833.1

Hsu, P.-C., Li, T., You, L., Gao, J., & Ren, H. (2015). A spatial-temporal projection model for 10–30 day rainfall forecast in South China. *Climate Dynamics*, *44*, 1227–1244. https://doi.org/10.1007/s00382-014-2215-4

Jiang, X., Xiang, B., Zhao, M., Li, T., Lin, S.-J., Wang, Z., & Chen, J.-H. (2018). Intraseasonal tropical cyclogenesis prediction in a global coupled model system. *Journal of Climate*, *31*, 6209–6227. https://doi.org/10.1175/JCLI-D-17-0454.1

Jolliffe, L. T., & Stephenson, D. B. (2005). FORECASTERS' FORUM comments on "discussion of verification concepts in forecast verification: A practitioner's guide in atmospheric science". *Weather and Forecasting*, *20*(5), 796–800. https://doi.org/10.1175/WAF877.1

Kim, H.-S., Kim, J.-H., Ho, C.-H., & Chu, P.-S. (2011). Pattern classification of typhoon tracks using the fuzzy *c*-means clustering method. *Journal of Climate*, *24*(2), 488–508. https://doi.org/10.1175/2010JCLI3751.1

Kim, H.-S., Kim, J.-H., Ho, C.-H., & Chu, P.-S. (2012). Track-pattern-based model for seasonal prediction of tropical cyclone activity in the Western North Pacific. *Journal of Climate*, *25*(13), 4660–4678. https://doi.org/10.1175/JCLI-D-11-00236.1

Lee, C.-Y., Camargo, S. J., Vitart, F., Sobel, A. H., Camp, J., Wang, S., et al. (2020). Subseasonal predictions of tropical cyclone occurrence and ACE in the S2S dataset. *Weather and Forecasting*, *35*, 921–938. https://doi.org/10.1175/WAF-D-19-0217.1

Lee, C.-Y., Camargo, S. J., Vitart, F., Sobel, A. H., & Tippett, M. K. (2018). Subseasonal tropical cyclone genesis prediction and MJO in the S2S dataset. *Weather and Forecasting*, *33*, 967–988. https://doi.org/10.1175/WAF-D-17-0165.1

Leroy, A., & Wheeler, M. C. (2008). Statistical prediction of weekly tropical cyclone activity in the southern hemisphere. *Monthly Weather Review*, *136*(10), 3637–3654. https://doi.org/10.1175/2008MWR2426.1

Li, R. C. Y., & Zhou, W. (2013). Modulation of western north pacific tropical cyclone activity by the ISO. Part II: Tracks and landfalls. *Journal of Climate*, *26*, 2919–2930. https://doi.org/10.1175/JCLI-D-12-00211.1

Li, W., Wang, Z., Zhang, G., Peng, M., Benjamin, S., & Zhao, M. (2018). Subseasonal variability of Rossby wave breaking and impacts on tropical cyclones during the North Atlantic warm season. *Journal of Climate*, *31*, 9679–9695. https://doi.org/10.1175/JCLID-17-0880.1

Liebmann, B., & Smith, C. A. (1996). Description of a complete (interpolated) outgoing longwave radiation dataset. *Bulletin of the American Meteorological Society*, *77*(6), 1275–1277.

Murakami, H., Villarini, G., Vecchi, G. A., Zhang, W., & Gudgel, R. (2016). Statistical–dynamical seasonal forecast of North Atlantic and U. S. landfalling tropical cyclones using the high-resolution GFDL FLOR coupled model. *Monthly Weather Review*, *144*, 2101–2123. https://doi.org/10.1175/MWR-D-15-0308.1

Qian, Y., Hsu, P.-C., & Kazuyoshi, K. (2019). New real-time indices for the quasi-biweekly oscillation over the Asian summer monsoon region. *Climate Dynamics*, *53*, 2603–2624. https://doi.org/10.1007/s00382-019-04644-0

Schreck, C. J., Molinari, J., & Aiyyer, A. (2012). A global view of equatorial waves and tropical cyclogenesis. *Monthly Weather Review*, *140*(3), 774–788. https://doi.org/10.1175/MWR-D-11-00110.1

Slade, S. A., & Maloney, E. D. (2013). An intraseasonal prediction model of Atlantic and East Pacific tropical cyclone genesis. *Monthly Weather Review*, *141*, 1925–1942. https://doi.org/10.1175/MWR-D-12-00268.1

Stanski, H. R., Wilson, L. J., & Burrowa, W. R. (1989). Survey of common verification methods in meteorology. World Weather Watch Tech Rep. 8, WMO Tech. Doc. 358, 114 pp.

Vecchi, G. A., Delworth, T., Gudgel, R., Kapnick, S., Rosati, A., Wittenberg, A. T., et al. (2014). On the seasonal forecasting of regional tropical cyclone activity. *Journal of Climate*, *27*, 7994–8016. https://doi.org/10.1175/JCLI-D-14-00158.1

Vitart, F., Ardilouze, C., Bonet, A., Brookshaw, A., Chen, M., Codorean, C., et al. (2017). The subseaasonal to seasonal (S2S) prediction project database. *Bulletin of the American Meteorological Society*, *98*, 163–173. https://doi.org/10.1175/BAMS-D-16-0017.1

Vitart, F., Leroy, A., & Wheeler, M. C. (2010). A comparison of dynamical and statistical predictions of weekly tropical cyclone activity in the southern hemisphere. *Monthly Weather Review*, *138*(9), 3671–3682. https://doi.org/10.1175/2010MWR3343.1

Vitart, F., Robertson, A. W., & Anderson, D. L. T. (2012). Subseasonal to seasonal prediction project: Bridging the gap between weather and climate. *WMO Bulletin*, *61*(2), 23–28.

Waliser, D. E. (2011). Predictability and forecasting. In W. K. M. Lau, & D. E. Waliser (Eds.), *Intraseasonal Variability of the Atmosphere-Ocean Climate System* (pp. 389–423). Berlin, Heidelberg: Springer. https://doi.org/10.1007/978-3-642-13914-7

Wheeler, M. C., & Hendon, H. H. (2004). An all-season real-time multivariate MJO index: Development of an index for monitoring and prediction. *Monthly Weather Review*, *132*(8), 1917–1932. https://doi.org/10.1175/1520-0493(2004)132,1917:AARMMI.2.0.CO;2

Wilks, D. S. (2006). *Statistical Methods in the Atmospheric Sciences* (2nd ed., pp. 294–298). London: Academic Press.

Xiang, B., Lin, S.-J., Zhao, M., Zhang, S., Vecchi, G., Li, T., et al. (2015). Beyond weather time-scale prediction for Hurricane Sandy and Super Typhoon Haiyan in a global climate model. *Monthly Weather Review*, *143*, 524–535. https://doi.org/10.1175/MWR-D-14-00227.1

Xiang, B., Zhao, M., Jiang, X., Lin, S.-J., Li, T., Fu, X., & Vecchi, G. (2015). The 3–4-week MJO prediction skill in a GFDL coupled model. *Journal of Climate*, *28*, 5351–5364. https://doi.org/10.1175/JCLI-D-15-0102.1

Zhang, G., Wang, Z., Peng, M., & Magnusdottir, G. (2017). Characteristics and impacts of extratropical Rossby wave breaking during the Atlantic hurricane season. *Journal of Climate*, *30*, 2363–2379. https://doi.org/10.1175/JCLI-D-16-0425.1

Zhang, H., Chu, P.-S., He, L., & Unger, D. (2019). Improving the CPC's ENSO forecasts using Bayesian model averaging. *Climate Dynamics*, *53*, 3373–3385. https://doi.org/10.1007/s00382-019-04710-7

Zhao, H., Jiang, X., & Wu, L. (2015). Modulation of northwest Pacific tropical cyclone genesis by the intraseasonal variability. *Journal of the Meteorological Society of Japan*, *93*, 81–97. https://doi.org/10.2151/jmsj.2015-006

Zhao, M., Golaz, J.-C., Held, I. M., Guo, H., Balaji, V., Benson, R., et al. (2018). The GFDL global atmosphere and land model AM4.0/LM4.0: 2. Model description, sensitivity studies, and tuning strategies. *Journal of Advances in Modeling Earth Systems*, *10*, 691–734. https://doi.org/10.1002/2017MS001208

References From the Supporting Information

Chaudhuri, S., Dutta, D., Goswami, S., & Middey, A. (2015). Track and intensity forecast of tropical cyclones over the North Indian Ocean with multilayer feed forward neural nets. *Meteorological Applications*, *22*(3), 563–575. https://doi.org/10.1002/met.1488

Harris, L. M., Lin, S.-J., & Tu, C. (2016). High-resolution climate simulations using GFDL HiRAM with a stretched global grid. *Journal of Climate*, *29*(11), 4293–4314. https://doi.org/10.1175/jcli-d-15-0389.1

Lee, J.-Y., Wang, B., Wheeler, M. C., Fu, X., Waliser, D. E., & Kang, I.-S. (2013). Real-time multivariate indices for the boreal summer intraseasonal oscillation over the Asian summer monsoon region. *Climate Dynamics*, *40*(1–2), 493–509. https://doi.org/10.1007/s00382-012-1544-4

Murakami, H., & Wang, B. (2010). Future change of North Atlantic tropical cyclone tracks: Projection by a 20-km-mesh global atmospheric model. *Journal of Climate*, *23*(10), 2699–2721. https://doi.org/10.1175/2010jcli3338.1